CHEMISTRY
A EUROPEAN JOURNAL

Supporting Information

Helical Hairpin Structure of a potent Antimicrobial Peptide MSI-594 in Lipopolysaccharide Micelles by NMR

Anirban Bhunia,[a] Ayyalusamy Ramamoorthy[b] and Surajit Bhattacharjya[a]

[a] *School of Biological Sciences, Nanyang Technological University, 60 Nanyang Drive, Singapore-637551*

[b] *Department of Chemistry and Biophysics, University of Michigan, Ann Arbor, MI 48109-1055*

NMR derived structure calculation: NMR structures of MSI-594 peptide bound to LPS were calculated using the DYANA program version 1.5[1]. On the basis of cross-peak intensities calculated using SPARKY program, T. D. Goddard and D. G. Kneller, University of California, San Francisco, from the TR-NOESY spectrum, recorded a with mixing time of 150 ms. The TR-NOE intensities were translated into strong, medium and weak to an upper bound distance limits to 2.5, 3.5 and 5.0 Å, respectively, as described in our earlier works[2]. Several round of structure calculations were carried out from random conformations, depending of NOE violations, distance constraints were adjusted. Backbone dihedral angle ϕ was restricted to -30^{o} to -120^{o} of non-glycyl residues to restrict conformational sampling. Out of the 100 structures generated, 20 lowest energy structures were used for further analysis. The structural statistics are provided in Table S3.

Relaxation dispersion experiments: The binding kinetics of MSI-594 to LPS was obtained from ^{1}H relaxation dispersion experiments using the Carr-Purcell-Meiboom-Gill (CPMG) pulse sequence[3] on a Bruker DRX 700 spectrometer, equipped with actively shielded cryo-probe and pulse field gradients. The nonselective 90° pulse (t_{90}=7.65 μs) was used to excite the sample and multiple non-selective 180° pulses (t_{180}~ 15.30 μs) generated the echo train. The relaxation dispersion profile was derived from the spectral peak intensities at different effective B_1 fields and the relaxation rates were fitted to the following equation to calculate the off-rate (k_{off}).[3]

$$R_2^{eff} = P_F R_{2,F} + P_B R_{2,B} + \left(\tau_b P_F P_B (\delta\omega)^2\right) * \left(1 - \frac{2\tau_b}{t_{cp}} \tanh[\frac{t_{cp}}{2\tau_b}]\right) \qquad \textbf{Equation 1}$$

Where, $\delta\omega$ is the chemical shift difference, P_F and P_B are mole fractions of free and bound peptide, respectively, and $R_{2,F}$ and $R_{2,B}$ are the relaxation rate of free and bound peptide, respective, t_{cp} is the delay and $k_{ex}=1/\tau_b$ (τ_b is the average life time in the bound state).

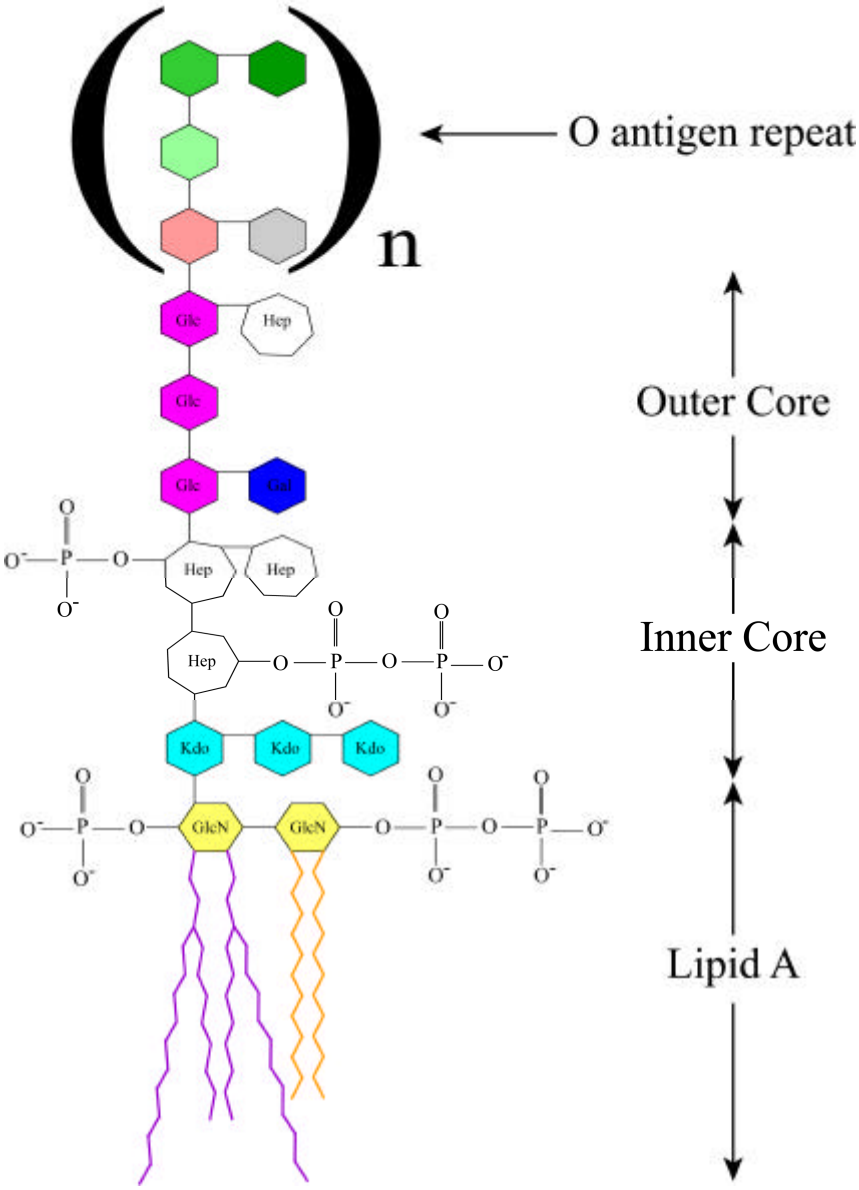

Scheme S1. Outer membrane of the Gram-negative bacteria contains LPS, which consists of outer core, inner core and lipid A. The phosphate group of lipid A, which is ~13 Å apart from the bis-phosphate groups, forms salt bridges with the positively charged amino acids of MSI-594.

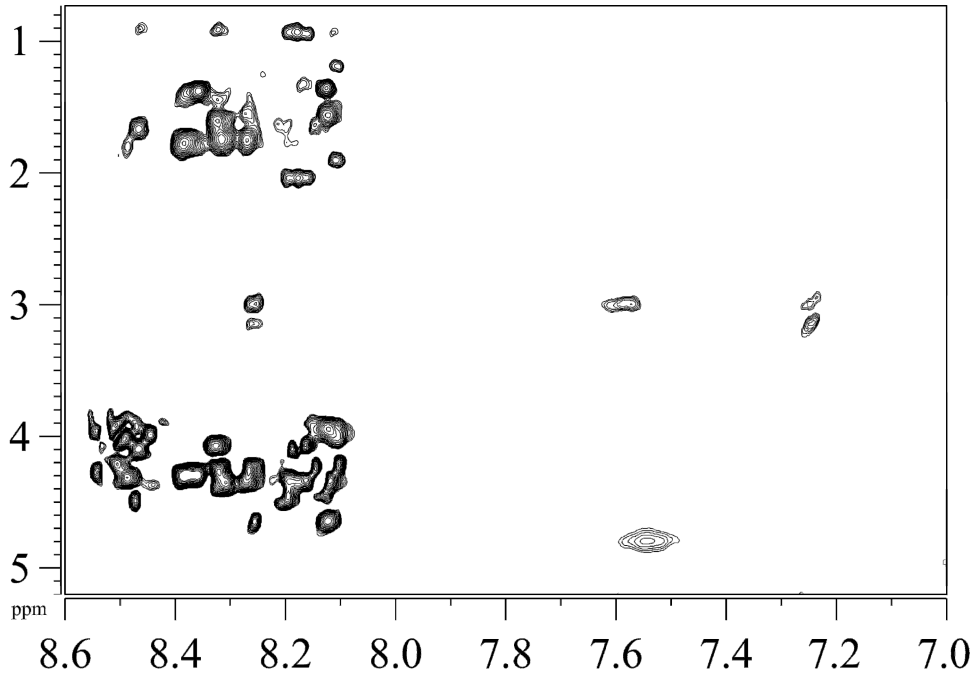

Figure S1. Expansion of the 2D ^{1}H-^{1}H NOESY spectrum of MSI-594 in aqueous solution (pH 4.8) at 298 K and at 600 MHz. As the correlation time (τ_c) of the molecule in aqueous solution is very fast, only sequential NOEs are observed.

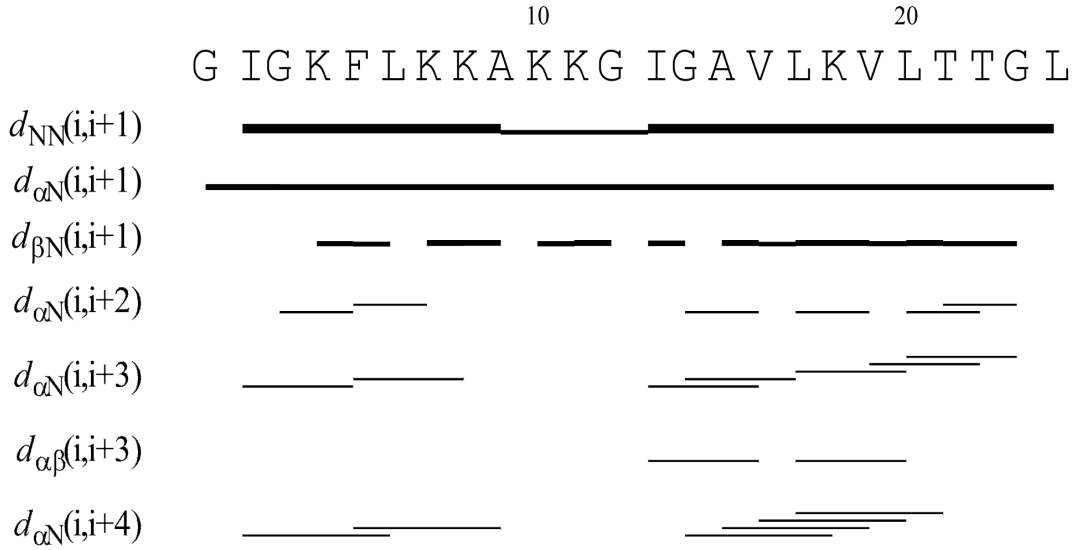

Figure S2. Bar diagram showing the summary of tr-NOEs of MSI-594 in the presence of either *E. coli* LPS or *S. typhimurium* LPS. The thickness of the bar diagram indicates the relative intensities of NOE cross peaks. Amino acid sequence of MSI-594 is shown at the top.

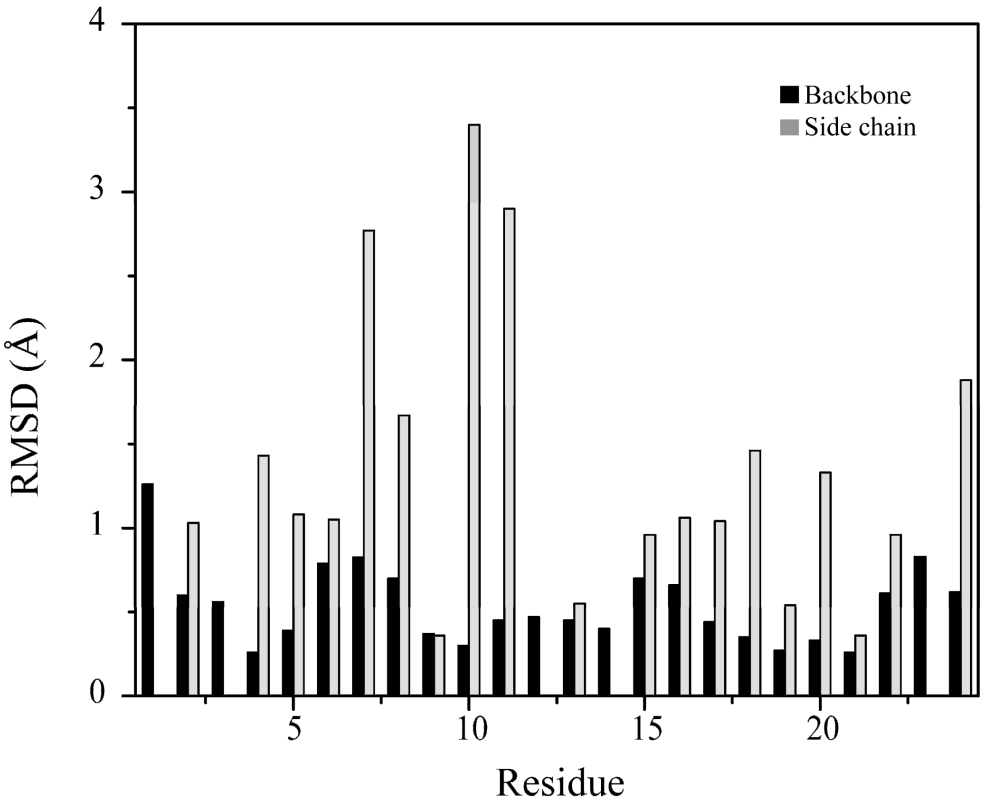

Figure S3. Root mean square deviations of the backbone and sidechain heavy atoms derived from the 20 lowest energy structures of MSI-594 in LPS.

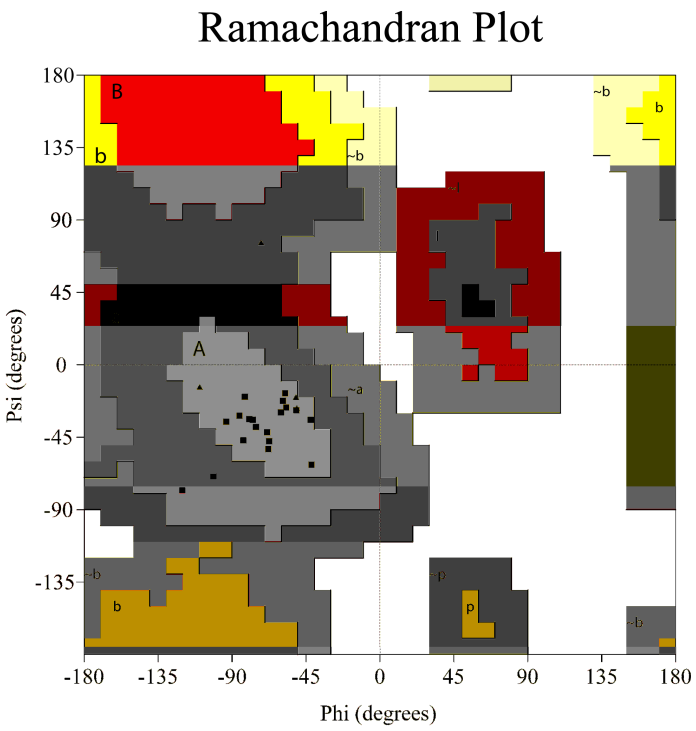

Plot statistics

Residues in most favoured regions [A,B,L]	16	89.5%
Residues in additional allowed regions [a,b,l,p]	2	10.5%
Residues in generously allowed regions [~a,~b,~l,~p]	0	0.0%
Residues in disallowed regions	0	0.0%
Number of non-glycine and non-proline residues	18	100.0%
Number of end-residues (excl. Gly and Pro)	0	
Number of glycine residues (shown as triangles)	6	
Number of proline residues	0	
Total number of residues	24	

Figure S4. The stereochemical quality of the ensemble of structures of MSI-594 in the presence of LPS was determined using program, PROCHECK-NMR.

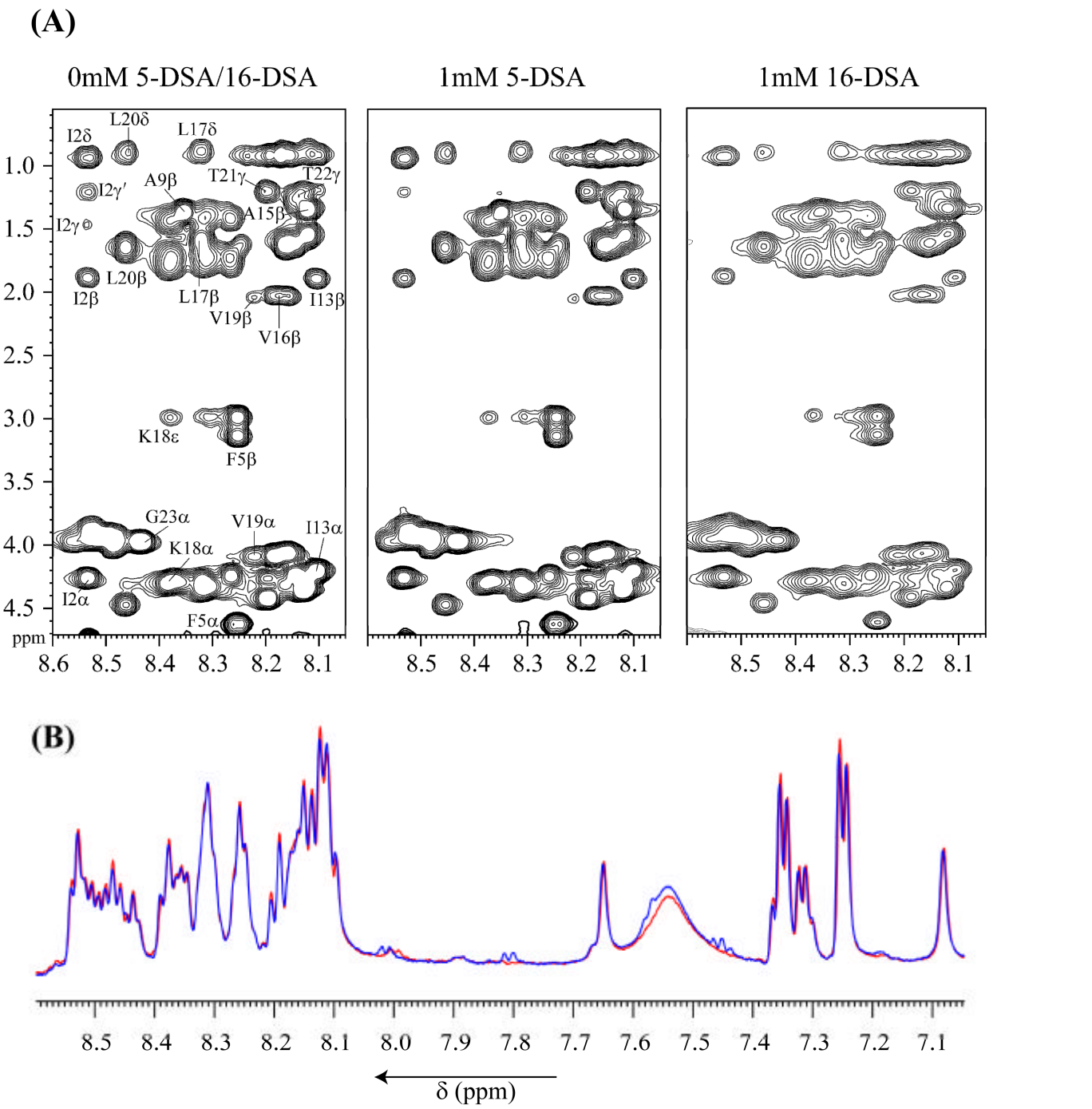

Figure S5. (A) Expansion of two-dimensional TOCSY NMR spectra of MSI-594 in the presence of 0.13 mg/mL LPS with or without the spin label, 5-DSA or 16-DSA. Line broadening is manifested by diminution of the cross peak intensities in the presence of either 5-DSA or 16-DSA. It is noteworthy that the positively charged amino acid surfaces of the MSI-594 is effected by 5-DSA (middle) due to its electrostatic interaction with the phosphate groups of LPS whereas the other face of MSI-594 bound to LPS is effected by 16-DSA because of its hydrophobic interaction with the acyl chain of LPS (right). (B) The expansion of 1D NMR spectrum of MSI-594 in aqueous solution (red colour) and in the presence of 1 mM of 5-DSA/16-DSA (blue colour). The control experiment clearly indicates that that spin label does not show line broadening on the peptide alone due to the fast tumbling of peptide.

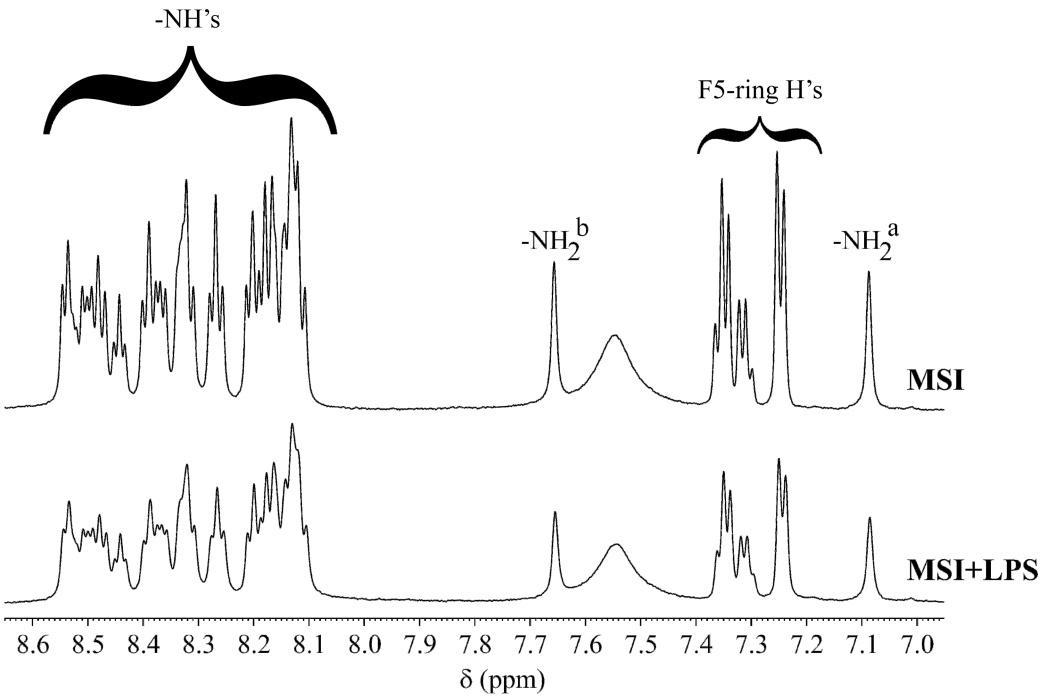

Figure S6. Low-field region of one-dimensional ^{1}H NMR spectra of MSI-594 in aqueous solution (pH 4.8) (top) and in the presence of *E.coli* LPS (0.13 mg/mL) (bottom). The spectrum of MSI-594 in the presence of *S. typhimurium* LPS (0.10mg/mL) is almost same as the bottom spectrum. Line-broadening effect (R2) of MSI-594 in the presence of LPS indicating that MSI-594 binds to the LPS (Table S1).

Table S1. The off-rate (k_{off}) and average life time (τ_b) at the bound state of MSI-LPS complex were obtained from the equation 1 from CPMG experiments. The equilibrium dissociation constant, K_d value, was estimated assuming k_{on} is under diffusion controlled (10^8 $M^{-1}S^{-1}$)

Sample	**R_2 (s^{-1})**	**K_D (mM)**	**t_b (ms)**	**k_{off} (s^{-1})**
MSI-594	1.28	n.a	n.a	n.a
LPS+MSI-594	8.33	71	140	7142

Table S2. The ^{1}H Chemical shifts (in ppm) of amino acid residues of MSI-594 in the presence of LPS (0.13 mg/mL) (90% H_20, 10% D_2O) at pH 4.8, 298 K and 600MHz. Chemical shifts were referenced to DSS.

Residue	**H_N**	**H_a**	**H_{b1}, H_{b2}**	**H_g**	**H_d**	**Others**
G1	-	3.78				
I2	8.54	4.27	1.90	1.47, 1.22	0.95	
G3	8.48	3.88, 3.95				
K4	8.16	4.33	1.64	1.46		$C^{\varepsilon}H$: 3.00 $N^{\varepsilon}H$: 7.55
F5	8.26	4.64	3.14, 3.00			2,6H: 7.24 3,5H: 7.35 4H : 7.31
L6	8.13	4.35	1.56		0.92	
K7	8.32	4.33	1.75			$C^{\varepsilon}H$: 2.99 $N^{\varepsilon}H$: 7.55
K8	8.27	4.25	1.71	1.44	1.56	$C^{\varepsilon}H$: 3.00 $N^{\varepsilon}H$: 7.55
A9	8.36	4.32	1.37			
K10	8.27	4.26	1.80		1.61	$N^{\varepsilon}H$: 7.55
K11	8.33	4.32	1.73	1.44		$C^{\varepsilon}H$: 3.00 $N^{\varepsilon}H$: 7.55
G12	8.49	4.02				
I13	8.11	4.22	1.90	1.46, 1.21	0.93	
G14	8.51	3.94				
A15	8.13	4.33	1.36			
V16	8.17	4.07	2.05	0.92		
L17	8.33	4.31	1.60		0.88	
K18	8.39	4.30	1.76	1.45		$C^{\varepsilon}H$: 3.00 $N^{\varepsilon}H$: 7.55
V19	8.20	4.09	2.04	0.93		
L20	8.47	4.48	1.65		0.90	
T21	8.20	4.43	4.26	1.21		
T22	8.14	4.36	4.25	1.21		
G23	8.46	3.94				
L24	8.15	4.31	1.64		0.93	

Table S3. Summary of structural statistics for the 20 final structures of LPS-bound MSI-594.

Distance restraints	
intraresidue (i - j = 0)	46
sequential (|i – j| = 1)	87
medium-range ($2 \leq \|i - j\| \leq 4$)	55
long-range ($\|i - j\| \geq 5$)	15
total	203
Angular restraints (f)	23
Distance restraints violations	
Number of violations	13
Average violation	$\leq$ 0.15 Å
Maximum violation	$\leq$ 0.40 Å
Deviation from mean structure	
All residues (N, C_α, C′)	0.38±0.10 Å
Heavy atoms	0.81±0.12 Å
Ramachandran plot for the mean structure	
% residues in the most favorable and additionally allowed region	100
% residues in the generously allowed region	0
% residues in the disallowed region	0

Table S4. Spin label induced line broadening of MSI-594 in the presence of LPS. The non-overlapping cross-peaks of MSI-594 in the presence of LPS were used for calculating the line broadening effect either by 5-DSA or by 16-DSA.

Residue	Cross peak	$I_{5\text{-DSA}}/I_{\text{no DSA}}$	$I_{16\text{-DSA}}/I_{\text{no DSA}}$	$I_{5\text{-DSA}}/I_{16\text{-DSA}}$
Ile2	$C^{\alpha}H$-NH	0.84	0.70	1.20
	$C^{\beta}H$-NH	0.85	0.69	1.23
	$C^{\gamma}Hs$-NH	0.79	0.71	1.11
	$C^{\delta}Hs$-NH	0.84	0.76	1.10
Phe5	$C^{\alpha}H$-NH	0.78	0.74	1.05
	$C^{\beta}Hs$-NH	0.83	0.73	1.14
Ala9	$C^{\beta}Hs$-NH	0.71	0.61	1.16
Ile13	$C^{\alpha}H$-NH	0.91	0.83	1.10
	$C^{\beta}H$-NH	0.77	0.67	1.15
Ala15	$C^{\beta}Hs$-NH	0.81	0.67	1.20
Val16	$C^{\beta}H$-NH	0.75	0.98	0.76
Leu17	$C^{\beta}Hs$-NH	1.14	0.80	1.42
	$C^{\delta}Hs$-NH	0.73	0.98	0.74
Lys18	$C^{\alpha}H$-NH	0.75	1.03	0.73
	$C^{\epsilon}Hs$-NH	0.74	1.22	0.60
Val19	$C^{\alpha}H$-NH	0.77	0.95	0.81
	$C^{\beta}H$-NH	0.76	1.02	0.74
Leu20	$C^{\alpha}H$-NH	0.78	0.83	0.94
	$C^{\beta}Hs$-NH	0.78	0.86	0.90
	$C^{\delta}Hs$-NH	0.78	1.49	0.52
Thr21	$C^{\gamma}H_3$-NH	0.77	0.90	0.85
Thr22	$C^{\gamma}H_3$-NH	0.70	0.90	0.77
Gly23	$C^{\alpha}H_2$-NH	0.90	0.82	1.10
Leu24	$C^{\beta}Hs$-NH	0.85	0.72	1.18

References:

(1) P. Guentert, C. Mumenthaler, K. Wuethrich, *J. Mol. Biol.* **1997**, *273*, 283-98.

(2) (a) A. Bhunia, G. L. Chua, P. N. Domadia, H. Warshakoon, J. R. Cromer, S. A .David, S. Bhattacharjya, *Biochem. Biophys. Res. Commun*., **2008**, *369*, 853-857. (b) S. Bhattacharjya, P. N. Domdia, A. Bhunia, S. Malladi, S. A. David, *Biochemistry*, **2007**, *46*, 5864-5874.

(3) (a) S. Meiboom, D. Gill, *Rev. Sci. Instrum.* **1958**, *29*, 688. (b) B. W. Dubois, A. S. Evers, *Biochemistry* **1992**, *31*, 7069-76. (c) B. Japelj, P. Pristovsek, A. Majerle, R. Jerala, *J. Biol. Chem.* **2005**, *280*, 16955-16961. (d) D. Tolkatchev, P. Xu, F. Ni, *J. Am. Chem. Soc.* **2003**, *125*, 12432-12442.